

SAS-6 defines a protein family required for centrosome duplication in *C. elegans* and in human cells

Sebastian Leidel¹, Marie Delattre¹, Lorenzo Cerutti², Karine Baumer¹ and Pierre Gönczy^{1,3}

The mechanisms that ensure centrosome duplication are poorly understood. In *Caenorhabditis elegans*, ZYG-1, SAS-4, SAS-5 and SPD-2 are required for centriole formation. However, it is unclear whether these proteins have functional homologues in other organisms. Here, we identify SAS-6 as a component that is required for daughter centriole formation in *C. elegans*. SAS-6 is a coiled-coil protein that is recruited to centrioles at the onset of the centrosome duplication cycle. Our analysis indicates that SAS-6 and SAS-5 associate and that this interaction, as well as ZYG-1 function, is required for SAS-6 centriolar recruitment. SAS-6 is the founding member of an evolutionarily conserved protein family that contains the novel PISA motif. We investigated the function of the human homologue of SAS-6. GFP-HsSAS-6 localizes to centrosomes and its overexpression results in excess foci-bearing centriolar markers. Furthermore, siRNA-mediated inactivation of HsSAS-6 in U2OS cells abrogates centrosome overduplication following aphidicolin treatment and interferes with the normal centrosome duplication cycle. Therefore, HsSAS-6 is also required for centrosome duplication, indicating that the function of SAS-6-related proteins has been widely conserved during evolution.

Centrosomes are the main microtubule-organizing centres (MTOCs) of animal cells and consist of a pair of centrioles surrounded by pericentriolar material (PCM). The single centrosome that is present early in the cell cycle duplicates during S phase to yield two centrosomes that organize a bipolar spindle during mitosis. Despite being crucial for cell division, the mechanisms that regulate centrosome duplication are not fully understood.

Genetic and functional genomic screens in *Caenorhabditis elegans* have led to the identification of four proteins that are essential for daughter centriole formation during the centrosome duplication cycle. Whereas ZYG-1 is a kinase that localizes to centrioles during mitosis only¹, SAS-4, SAS-5 and SPD-2 are coiled-coil proteins that localize to centrioles throughout the cell cycle^{2–6}. Fluorescence recovery after photobleaching (FRAP) experiments show that SAS-4 is recruited to centrioles once per cell cycle; this occurs at the onset of the duplication cycle³. Marked mating experiments, in which the sperm contributes unlabelled centrioles to an oocyte expressing green fluorescent protein (GFP)-SAS-4, further indicate that SAS-4 is incorporated into daughter centrioles^{2,3}. By contrast, centriolar SAS-5 exchanges with a cytoplasmic pool throughout the cell cycle⁴ and its presence at centrioles requires ZYG-1.

The extent to which findings in *C. elegans* can contribute to unravelling the mechanisms of centrosome duplication in other metazoans is a matter of some debate⁷. Centrioles in *C. elegans* are structurally divergent⁸, consisting of a radial array of nine singlet microtubules instead of the canonical nine triplet arrangement, and are ~100 × 100 nm

instead of ~150 × 400 nm in vertebrate cells. Moreover, the *C. elegans* genome does not encode a bona fide centrin, δ-tubulin or ε-tubulin, all of which are required for centriole or basal-body reproduction in other species^{7,9–12}. Conversely, other than in nematodes, there are no apparent homologues of ZYG-1 or SAS-5. Nevertheless, it has been suggested that distant relatives of SAS-4 and SPD-2 may be present in other metazoans^{3,6}. CPAP, the putative human relative of SAS-4, localizes to centrosomes and is involved in microtubule nucleation¹³, whereas both CPAP and the putative human relative of SPD-2 have been detected in a proteomic analysis of human centrosomes¹⁴. However, it remains to be established whether these components are involved in centrosome duplication. Therefore, whether *C. elegans* will be instrumental in identifying evolutionarily conserved proteins of the centrosome duplication cycle remains an open question.

RESULTS

sas-6 is required for centrosome duplication in *C. elegans*

To identify novel components that are required for centrosome duplication in *C. elegans*, we sought to find genes whose inactivation by RNA interference (RNAi) results in defective spindle assembly in early embryos. Our analysis of two large data sets^{15,16} identified one such novel gene, Y45F10D.9, which we termed *sas-6*.

To analyse *sas-6*(RNAi) embryos, we performed dual differential interference contrast (DIC) and fluorescence time-lapse microscopy using transgenic animals expressing the PCM marker GFP-TAC-1 (ref. 17). In wild-type animals (Supplementary

¹Swiss Institute for Experimental Cancer Research (ISREC), CH-1066 Epalinges/Lausanne, Switzerland. ²Swiss Institute for Bioinformatics (SIB), CH-1066 Epalinges/Lausanne, Switzerland.

³Correspondence should be addressed to P.G. (Pierre.Gonczi@isrec.unil.ch)

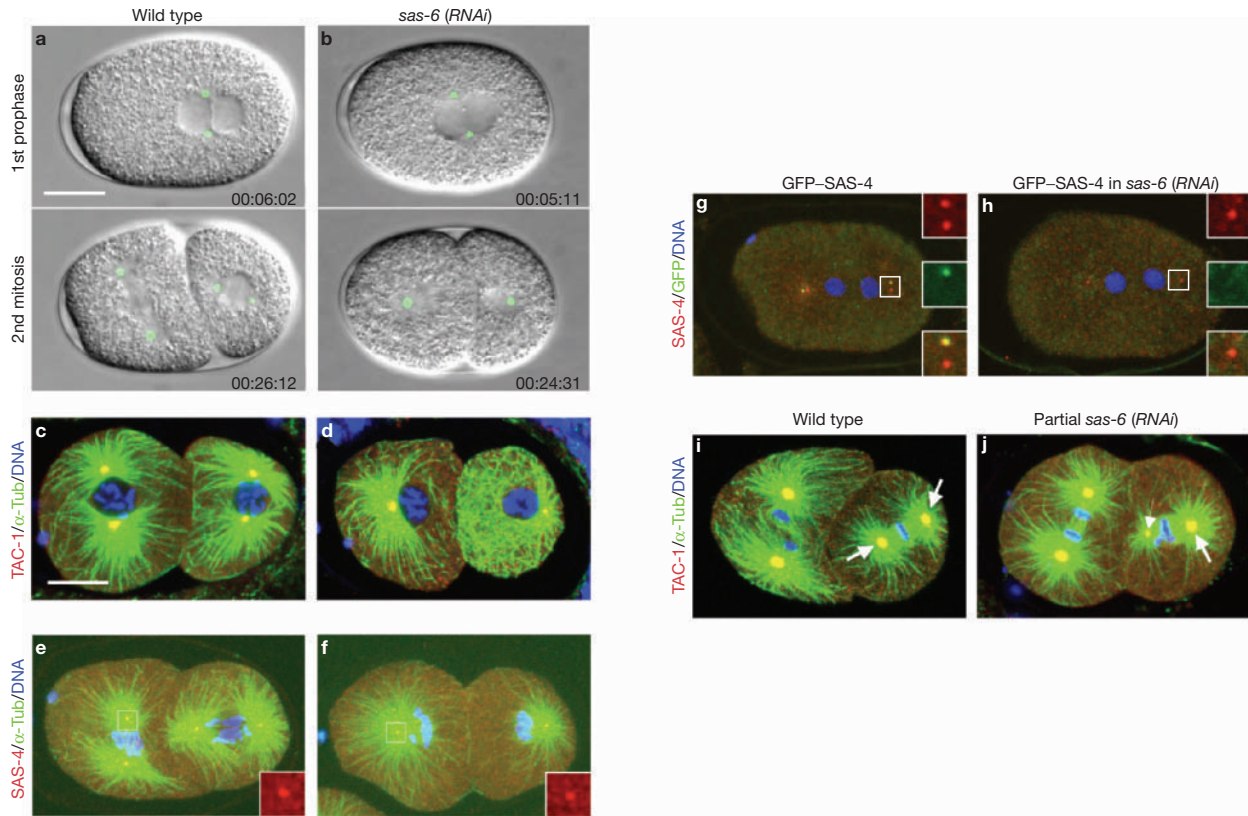


Figure 1 *sas-6* is required for daughter centriole formation. **(a, b)** Images from dual green fluorescent protein (GFP) fluorescence and differential interference contrast (DIC) time-lapse microscopy of wild-type (**a**) and *sas-6(RNAi)* (**b**) embryos expressing GFP-TAC-1 (see Supplementary information Movies 1 and 2). The GFP signal (green) is overlaid on the DIC image. Represented are embryos during prophase in the first cell cycle (top panels) and the second cell cycle (bottom panels). Elapsed time is shown in h, min and s. In this and other figures, anterior is to the left, posterior to the right, scale bars are 10 μm, and all panels of a kind are at the same magnification. **(c–f)** Wild-type (**c, e**) and *sas-6(RNAi)* (**d, f**) embryos at the two-cell stage are stained with antibodies against TAC-1 (**c, d**) or SAS-4 (**e, f**) (both red), as well as α-tubulin (α-TUB; green); DNA is shown in blue. In these and other figures, insets are threefold magnified views of one centrosome, unless stated otherwise. **(g, h)** Telophase one-cell-stage embryos resulting from a

fem-1(hc17) (**g**) or *fem-1(hc17) sas-6(RNAi)* (**h**) oocyte expressing GFP-SAS-4 fertilized by wild-type sperm; embryos were stained with antibodies against SAS-4 (red) and GFP (green); DNA is shown in blue. The presence of *fem-1(hc17)*, which confers a temperature-sensitive self-sterile phenotype to hermaphrodites²⁷, ensures that only cross-fertilization events are scored. Note that 1/2 centrioles per spindle pole has incorporated GFP-SAS-4 in the wild type (see also refs 2,3). **(i, j)** Two-cell-stage embryos from the wild type (**i**) or following partial RNAi-mediated inactivation of *sas-6* (**j**) stained with antibodies against TAC-1 (red) as well as α-tubulin (green); DNA is shown in blue. A projection of seven 0.5 μm confocal optical sections that encompasses all centrosomes is shown in (**j**). An asymmetry in centrosome size was observed in ~5% of blastomeres that were analysed at the two-cell stage ($n=204$). We noted also that the extent of asymmetry is typically less pronounced than that observed in *sas-4(RNAi)* embryos².

information Movie 1), centrosome duplication yields two centrosomes, which assemble a bipolar spindle at the one-cell stage (Fig. 1a, top) and in each blastomere at the two-cell stage (Fig. 1a, bottom). In *sas-6(RNAi)* embryos (Supplementary information Movie 2), whereas two MTOCs are apparent during mitosis at the one-cell stage (Fig. 1b, top), a single MTOC is observed in each blastomere at the two-cell stage (Fig. 1b, bottom). Immunofluorescence analysis confirmed that this MTOC contains one focus of TAC-1 (Fig. 1d, compare with Fig. 1c) and established that it harbours one focus of SAS-4 (Fig. 1f, compare with Fig. 1e), the size of which does not increase in subsequent cell cycles (data not shown).

An indistinguishable phenotype is observed in mutant embryos that lack maternal *zyg-1* or *sas-5* function^{1,4}, as well as in *sas-4(RNAi)* embryos^{2,3}, which also lack maternal function because sperm is not targeted by RNAi. In this case, as well as in *spd-2(RNAi)* embryos, the two paternally contributed centrioles split in the one-cell stage such that each centriole organizes one functional MTOC^{2,6}. However, MTOC duplication fails at the two-cell stage

because each single centriole cannot reproduce further. We tested whether *sas-6* is also required for daughter centriole formation using GFP-SAS-4 incorporation as an assay^{2–4}. When wild-type sperm contributes unlabelled centrioles to an oocyte expressing GFP-SAS-4, centrosomes in the resulting embryo normally bear GFP-positive centrioles after the first occurrence of daughter centriole formation (Fig. 1g; 11/11 embryos). By contrast, we found that when wild-type sperm contributes unlabelled centrioles to a *sas-6(RNAi)* oocyte expressing GFP-SAS-4, centrosomes in the resulting embryo never harbour GFP (Fig. 1h, 0/60 embryos), indicating that *sas-6* is required for daughter centriole formation.

sas-4, *zyg-1* and *sas-5* are dose-dependent regulators of centrosome duplication, in that their partial inactivation yields embryos at the two-cell stage with asymmetric spindles that have one normal spindle pole and one smaller spindle pole with a structurally compromised centriole^{2,4}. We found that partial RNAi-mediated inactivation of *sas-6* results in analogous intermediate phenotypes (Fig. 1j, compare

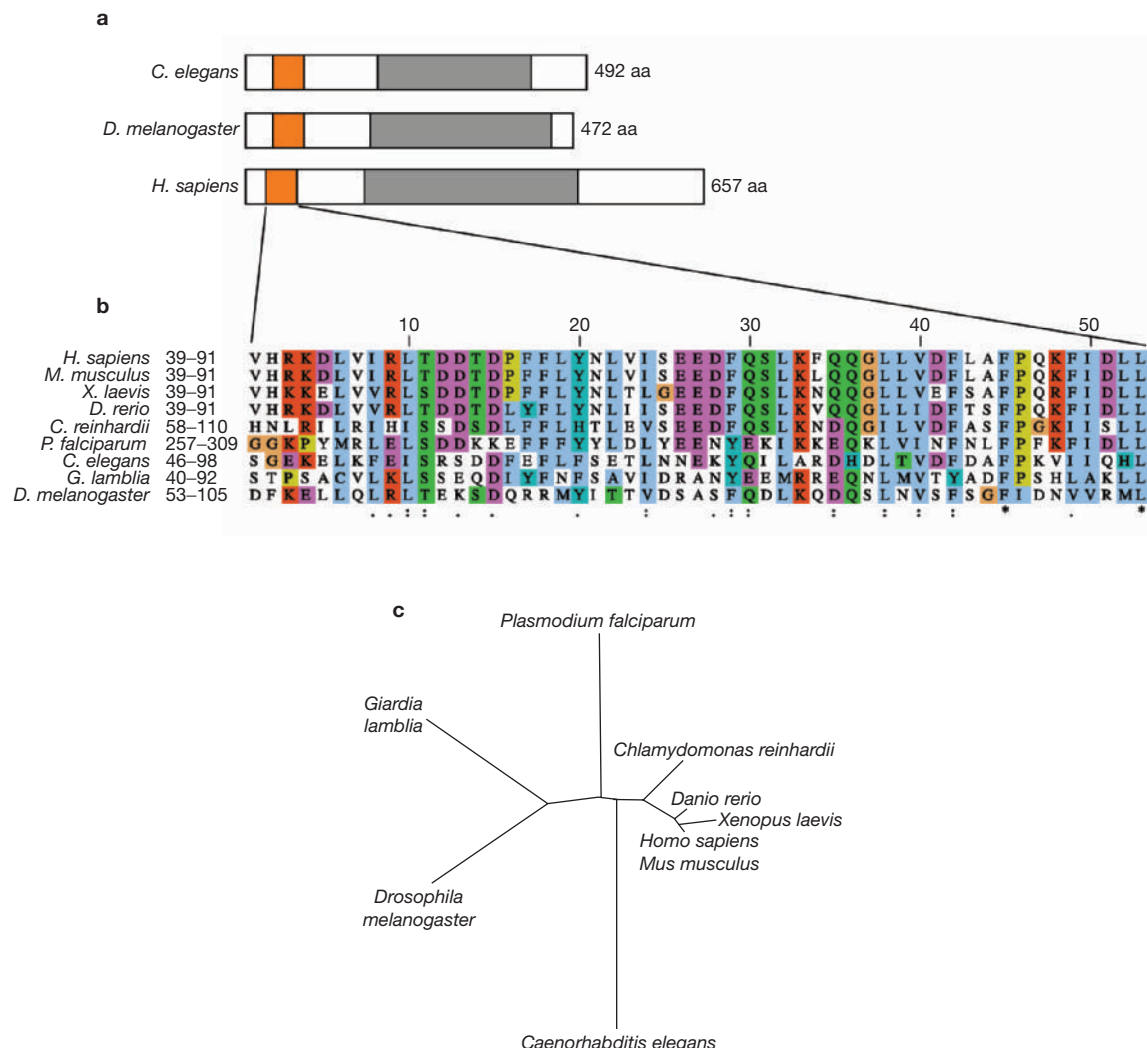


Figure 2 SAS-6 is the founding member of the conserved PISA-containing protein family. **(a)** Schematic representation of *Caenorhabditis elegans* (*C.e*) SAS-6 and related predicted proteins in *Drosophila melanogaster* (*D.m*) and *Homo Sapiens* (*H.s*). The conserved PISA motif is indicated in orange, the predicted coiled-coil domain in grey. Amino-acid (aa) identities are as follows. Full-length: *C.e* versus *D.m*: 18%; *C.e* versus *H.s*: 21%; *D.m* versus *H.s*: 19%. PISA motif: *C.e* versus *D.m*: 17%; *C.e* versus *H.s*: 28%; *D.m* versus *H.s*: 23%. Coiled-coil: *C.e* versus *D.m*: 21%; *C.e* versus *H.s*: 20%; *D.m* versus *H.s*: 23%. **(b)** Alignment of the ~50 amino-acid PISA motif found in TrEMBL sequences: *H. sapiens* (Q6UVJ0), *Mus musculus* (Q80UK7), *Xenopus laevis* (Q6NRG6), *Danio rerio* (Q7ZVT3), *Chlamydomonas reinhardtii* (predicted protein; see Methods), *Plasmodium falciparum* (Q6LFJ0), *C. elegans* (O62479), *Giardia lamblia* (Q7R0K5), *D. melanogaster* (Q9VAC8). Coordinates of

with Fig. 1i), indicating that *sas-6* is also a dose-dependent regulator of centrosome duplication.

SAS-6 is a member of an evolutionarily conserved protein family

SAS-6 is a protein that consists of 492 amino acids and has one predicted coiled-coil domain (Fig. 2a; see Methods). Using iterative Blast with the segment amino-terminal of the coiled-coil domain, we found a ~50 amino-acid region of homology in other organisms; we called this region the PISA (present in SAS-6) motif. By deriving a profile from the multiple alignment and using this to search for other

the PISA motif within the protein are indicated. Alignments are coloured using the ClustalX scheme in Jalview³⁶. Orange: glycine (G); gold: proline (P); blue: small and hydrophobic amino acids (A,V,L,I,M,F,W); green: hydroxyl and amine amino acids (S,T,N,Q); magenta: negatively charged amino acids (D,E); red: positively charged amino acids (R,K); dark blue: histidine (H) and tyrosine (Y). Identical residues (*), residues conserved in size and hydrophobicity/hydrophilicity (:), and residues conserved in size or hydrophobicity/hydrophilicity (.) are indicated. **(c)** Tree showing the relative distance among PISA motifs in select organisms, constructed using the programs from the phylip package (<http://evolution.genetics.washington.edu/phylip.html>). 100 bootstraps were generated using seqboot and used to compute a distance matrix with prodist (default parameters). The tree was constructed using the Fitch–Margoliash method with 10 randomized input orders and plotted using drawtree.

proteins containing this motif, we identified one PISA-containing protein in various organisms, including *Drosophila melanogaster* and *Homo sapiens* (Fig. 2a, 2b). Whereas no apparent PISA-containing protein is present in *Saccharomyces cerevisiae* or *Schizosaccharomyces pombe*, we identified one such protein in the protists *Plasmodium falciparum* and *Giardia lamblia*. This indicates that PISA-containing proteins have an ancient origin (Fig. 2b, 2c). Members of this protein family have a relatively conserved size and structure, with the PISA motif located towards the N terminus, followed by one predicted coiled-coil domain (Fig. 2a). Whereas functional analysis of other

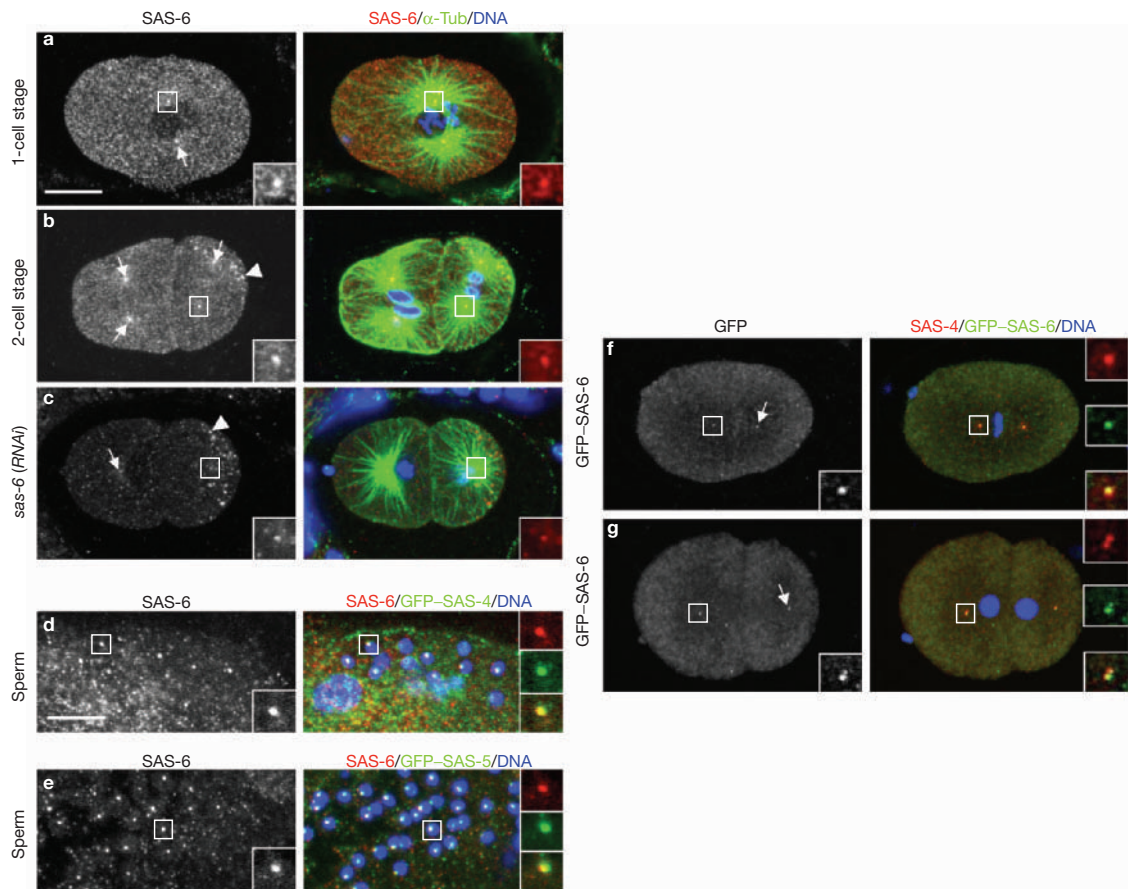


Figure 3 SAS-6 localizes to centrioles. (a–c) One-cell-stage (a) or two-cell-stage (b) wild-type embryos, as well as *sas-6(RNAi)* embryo (c) stained with antibodies against SAS-6 (shown alone on the left and in red in the merge) and α -tubulin (α -TUB; green); DNA is shown in blue. Note that SAS-6 antibodies also recognize P granules (b, arrowhead), but this aspect of the staining is not specific as it is still present in *sas-6(RNAi)* embryos (c, arrowhead). Arrows in this and other figures point to centrosomes that are not shown in the insets. (d, e) Sperm cells expressing green fluorescent protein (GFP)-SAS-4 (d) or GFP-SAS-5 (e) and stained with antibodies against SAS-6 (shown alone on the left and

PISA-containing proteins has not been performed before this work was carried out, the human SAS-6 protein has been found during a proteomic analysis of centrosomal components¹⁴.

SAS-6 is present at centrioles

We raised antibodies against *C. elegans* SAS-6 that recognize a single band of the predicted size in wild-type embryonic extracts, which is severely diminished in *sas-6(RNAi)* embryonic extracts (Fig. 6c). These antibodies preferentially label a dot in the centre of the centrosome in early embryos, as well as in the cytoplasm to a lesser extent (Fig. 3a, 3b). The signal is vastly diminished in *sas-6(RNAi)* embryos, indicating specificity (Fig. 3c). Furthermore, we found that SAS-6 colocalizes with GFP-SAS-4 and GFP-SAS-5 in sperm cells (Fig. 3d, 3e). We noted also that the distribution of SAS-6 appears to be more restricted than that of either fusion protein (insets, Fig. 3d, 3e), indicating that SAS-6 may be present in only part of the centrioles, although immunoelectron microscopy will be needed to ascertain this point. Overall, we conclude that SAS-6 is a component that is associated with centrioles.

in red in the merge) and GFP (green); DNA is shown in blue. (f) One-cell-stage embryo expressing GFP-SAS-6 and stained with antibodies against SAS-4 (red) and GFP (shown alone on the left and in green in the merge); DNA is shown in blue. (g) Late telophase one-cell-stage embryo from a cross between wild-type males and GFP-SAS-6 expressing hermaphrodites stained with antibodies against SAS-4 (red) and GFP (shown alone on the left and in green in the merge); DNA is shown in blue. Although GFP-SAS-6 is essentially not detectable in sperm cells (see Methods), the cross ensures that no trace GFP-SAS-6 is contributed by paternally-derived centrioles.

We generated transgenic animals expressing GFP-SAS-6. Staining of transgenic embryos with GFP antibodies confirmed the centriolar enrichment, as well as the cytoplasmic distribution (Fig. 3f). As expected, GFP-SAS-6 colocalizes with the centriolar component SAS-4 (Fig. 3f). We found an analogous distribution when filming GFP-SAS-6 embryos using spinning disc confocal microscopy (Fig. 4a, Supplementary information Movie 3). Quantification of fluorescence intensity in such recordings established that levels of centriolar GFP-SAS-6 remain constant throughout the cell cycle (Fig. 4c).

SAS-6 is recruited to centrioles once per cell cycle

We next examined the dynamics of GFP-SAS-6 recruitment to centrioles using FRAP analysis. We photobleached one centrosome at different time points in embryos at the one-cell stage, and assayed fluorescence recovery using four-dimensional confocal microscopy. Strikingly, we found that centriolar fluorescence recovery always occurs shortly after cytokinesis, irrespective of when photobleaching takes place (Fig. 4b, 4d). This time corresponds to the beginning of the duplication cycle in these embryonic cells, which oscillate between M and S phases^{2,3}.

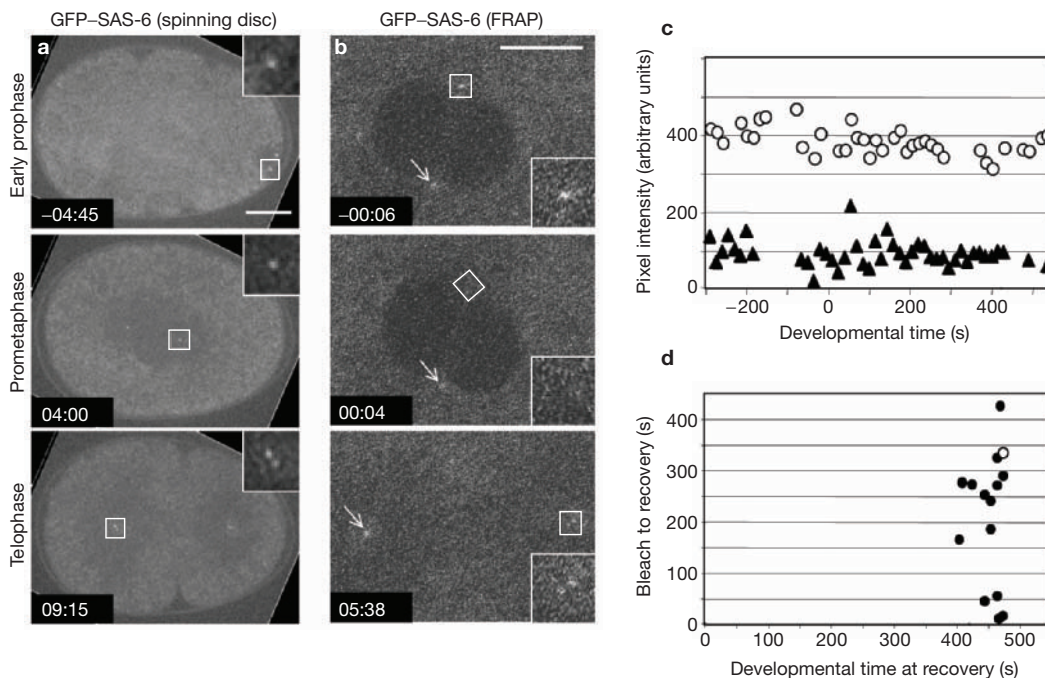


Figure 4 SAS-6 is recruited to centrioles once per cell cycle. **(a)** Images from spinning disc confocal time-lapse fluorescence microscopy of an embryo at the one-cell stage expressing GFP-SAS-6 at the indicated stages (see Supplementary information Movie 3). Elapsed time is shown in min and s, with 00:00 corresponding to pronuclear meeting. Note that the images extracted from Supplementary information Movie 3 have been rotated, resulting in the presence of black triangles on the panel edges. Note also that the ratio of centriolar/cytoplasmic signal is lower for GFP-SAS-6 than for GFP-SAS-4 or GFP-SAS-5 (refs 2–4). **(b)** Fluorescence recovery after photobleaching of GFP-SAS-6. Projections of two 1 μm confocal sections from an embryo at the one-cell stage before photobleaching (top), immediately after photobleaching (middle, white square indicates

Therefore, GFP-SAS-6 is recruited to centrioles once per cell cycle, at the onset of the duplication cycle.

We sought to determine whether GFP-SAS-6 is recruited to one or both centrioles by examining telophase one-cell-stage embryos. This time corresponds to the onset of the second duplication cycle, when each pair of parental centrioles splits such that the two centrioles become distinguishable as single entities. This allows assays to be performed to determine whether the two centrioles incorporated GFP-SAS-6 during the first duplication cycle, given that GFP-SAS-6 is absent from sperm (see Methods). We found that both centrioles of each pair harbour GFP-SAS-6 in telophase one-cell-stage embryos, with one centriole often showing a stronger signal when examined just after splitting (Fig. 3g). It therefore seems that GFP-SAS-6 associates with both mother and daughter centrioles during the duplication cycle. Alternatively, GFP-SAS-6 may be recruited primarily to the centriole that harbours the strongest signal by the end of the one-cell stage, with labelling of the other centriole reflecting a slow exchange with the cytoplasmic pool that is not detected by FRAP analysis. Another possibility is that the strongly labelled centriole recruited GFP-SAS-6 during the first duplication cycle, and began recruiting GFP-SAS-6 at the second duplication cycle, before splitting occurs. The other centriole began recruiting GFP-SAS-6 at the second duplication cycle.

targeted area, which is rotated rightwards in the inset) and at onset of recovery (bottom, note two foci of green fluorescent protein). Elapsed time is indicated in min and s with 00:00 corresponding to the end of photobleaching (the indicated time corresponds to that of the optical section in the middle of the stack). Arrows point to an unbleached centrosome. **(c)** Quantification of pixel intensities (arbitrary units) at both centrosomes in spinning disc confocal stack of embryo shown in **a**. 0 s: pronuclear meeting; 420 s: cytokinesis; indicated times correspond to that of the first image in the stack. For display convenience, values of the second centrosome are shifted up by 300 arbitrary units. **(d)** Time interval between bleach and recovery of GFP-SAS-6 as a function of developmental time at recovery (0 s: pronuclear meeting). White disc corresponds to embryo shown in **b**.

To independently assess whether GFP-SAS-6 is recruited to the mother centriole, we examined *sas-4(RNAi)* embryos, in which only mother centrioles are present because daughter centriole formation does not occur². As shown in Fig. 5b, we found that GFP-SAS-6 is present at centrioles in such embryos. Therefore, GFP-SAS-6 is recruited to the mother centriole or a closely associated structure. Interestingly, analysis of GFP-SAS-6 distribution throughout the cell cycle in *sas-4(RNAi)* embryos revealed that the protein is not present at centrioles between late prophase and early telophase (Fig. 5c, 5d). By contrast, centriolar GFP-SAS-6 is present throughout the cell cycle in otherwise wild-type embryos (Fig. 4a, 5a). Therefore, daughter centriole formation or *sas-4* function is required for persistence of GFP-SAS-6 at centrioles.

These observations prompted us to consider whether SAS-6 may be first recruited to the mother centriole and then associate in a stable manner with the daughter centriole that emanates from it, with only the second phase being affected by the absence of *sas-4*. Compatible with SAS-6 being associated in a stable manner with centrioles, we found that endogenous SAS-6 is present throughout the cell cycle in *sas-4(RNAi)* embryos (Fig. 5e), presumably reflecting the presence of SAS-6 on paternally contributed centrioles. Taken together, our observations lead us to propose that SAS-6 is recruited to the mother centriole or a closely associated structure at the onset of the centrosome duplication cycle and then associates with the emerging daughter centriole.

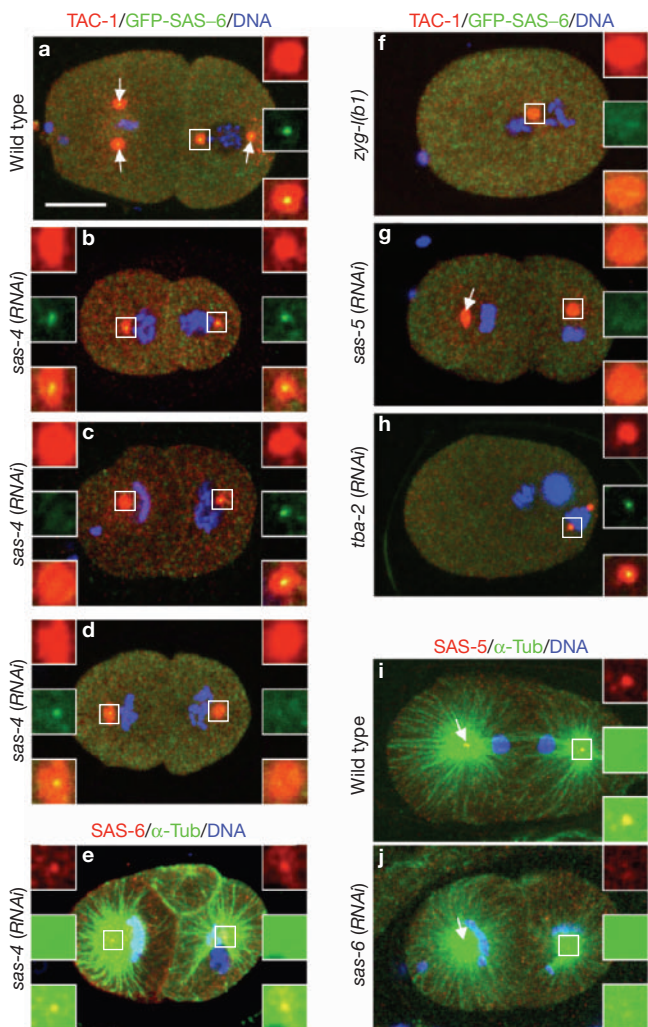


Figure 5 SAS-6 centriolar targeting. **(a–d)** Two-cell-stage wild-type (**a**) or *sas-4(RNAi)* (**b–d**) embryos expressing GFP-SAS-6 and stained with antibodies against TAC-1 (red) and green fluorescent protein (GFP; green); DNA is shown in blue. In the *sas-4(RNAi)* embryos, note that centrosomes harbour GFP-SAS-6 only when cells are in interphase. In **b**, both anterior (AB) and posterior (P_1) blastomeres are in interphase; in **c**, only P_1 is in interphase, whereas AB is already in mitosis at this stage; in **d**, AB has advanced to just after telophase, whereas P_1 is in mitosis in turn. **(e)** Two-cell-stage *sas-4(RNAi)* embryo stained with antibodies against SAS-6 (red) and α -tubulin (α -TUB; green); DNA is shown in blue. Note that centriolar SAS-6 is present in both blastomeres, including in the anterior blastomere AB, which is in mitosis. **(f–h)** *zyg-1(b1)* one-cell-stage (**f**), *sas-5(RNAi)* two-cell-stage (**g**) and *tba-2(RNAi)* (**h**) one-cell-stage embryos stained with antibodies against TAC-1 (red) and GFP-SAS-6 (green); DNA is shown in blue. **(i, j)** Wild-type one-cell-stage (**i**) and *sas-6(RNAi)* two-cell-stage (**j**) embryos stained with antibodies against SAS-5 (red) and α -tubulin (α -TUB; green); DNA is shown in blue.

Centriolar targeting of SAS-6

We next investigated whether other genes that are required for daughter centriole formation contribute to SAS-6 centriolar targeting. As shown in Fig. 5f and 5g, we found that centriolar GFP-SAS-6 is strikingly reduced in the absence of *zyg-1* or *sas-5* function. Conversely, levels of centriolar SAS-5 are significantly diminished compared with the wild type in *sas-6(RNAi)* embryos (Fig. 5j, compare with Fig. 5i). Similar conclusions were reached by filming GFP-SAS-6 in *zyg-1(RNAi)* embryos and GFP-SAS-5 in *sas-6(RNAi)* embryos (data not shown).

Western blot analysis indicates that overall levels of SAS-5 are not diminished in *sas-6(RNAi)* embryos, nor are those of SAS-6 in *sas-5(RNAi)* embryos (data not shown). The lack of GFP-SAS-6 at centrioles in *zyg-1(b1)* or *sas-5(RNAi)* embryos is unlikely to be due merely to a single centriole being present per centrosome, because centriolar GFP-SAS-6 is present in *sas-4(RNAi)* interphase embryos (Fig. 5b). Centriolar GFP-SAS-6 is also present in *tba-2(RNAi)* embryos, which presumably also bear a single mother centriole per centrosome due to depletion of tubulin dimers (Fig. 5h). This result also indicates that GFP-SAS-6 centriolar recruitment does not require microtubules. Overall, we conclude that ZYG-1 is required for the presence of SAS-6 at centrioles, and that SAS-6 and SAS-5 are dependent on one another for their centriolar distribution.

SAS-6 physically interacts with SAS-5

Because of the mutual relationships of SAS-6 and SAS-5, we investigated whether the proteins interact. Using a yeast two-hybrid assay, we found a robust interaction between SAS-6 and SAS-5 (Fig. 6a). Furthermore, we established that the coiled-coil domain of SAS-6 is sufficient and necessary for interaction with SAS-5 (Fig. 6b). In addition, we found that the interaction between SAS-6 and SAS-5 is markedly diminished when using SAS-5 corresponding to the *sas-5(t2079)* mutant allele (Fig. 6a), which has a single amino-acid substitution in the carboxy-terminal part of the protein⁴. This indicates that this residue is important for interaction with SAS-6 and raises the possibility that the observed failure of SAS-5[t2079] to localize to centrioles⁴ is due to lack of interaction with SAS-6.

To test if SAS-6 associates with SAS-5 *in vivo*, we set out to perform co-immunoprecipitation experiments. We affinity-purified antibodies against SAS-5 that were suitable for western blot analysis. These antibodies recognized two main species in wild-type embryonic extracts: one at the expected relative molecular mass (M_r) of ~56,000 (56K) and one at ~ M_r 35K. Both species are markedly reduced in *sas-5(RNAi)* mutant embryonic extracts, indicating specificity (Fig. 6d). We did not detect alternative splicing of *sas-5* (data not shown), indicating that the smaller species reflects a cleavage product of SAS-5. Importantly, we found that SAS-6 antibodies co-immunoprecipitate both species of SAS-5 (Fig. 6e), whereas this was not the case when using control antibodies (data not shown). Furthermore, we noted that a significant fraction of SAS-5 is immunoprecipitated by the SAS-6 antibodies (Fig. 6e). As the bulk of SAS-5 and SAS-6 is cytoplasmic⁴ (see Fig. 3), this result indicates that association between SAS-6 and SAS-5 already occurs in the cytoplasm.

HsSAS-6 is required for centrosome duplication in human cells

We set out to investigate whether the human homologue of SAS-6 is related in function to its *C. elegans* counterpart. We first addressed whether the HsSAS-6 localizes to centrosomes, as indicated by its detection in a proteomic analysis of the human centrosome¹⁴. We isolated a full-length HsSAS-6 cDNA, fused it to GFP, and transfected GFP-HsSAS-6 into U2OS cells. We found that GFP-HsSAS-6 is present at centrosomes, as judged by colocalization with γ -tubulin, the centriolar proteins C-Nap1 and centrin-3, as well as poly-glutamylated tubulin, a stable tubulin isoform that marks centrioles¹⁸ (Fig. 7a–e). These observations further ascertain that HsSAS-6 is a centrosomal protein.

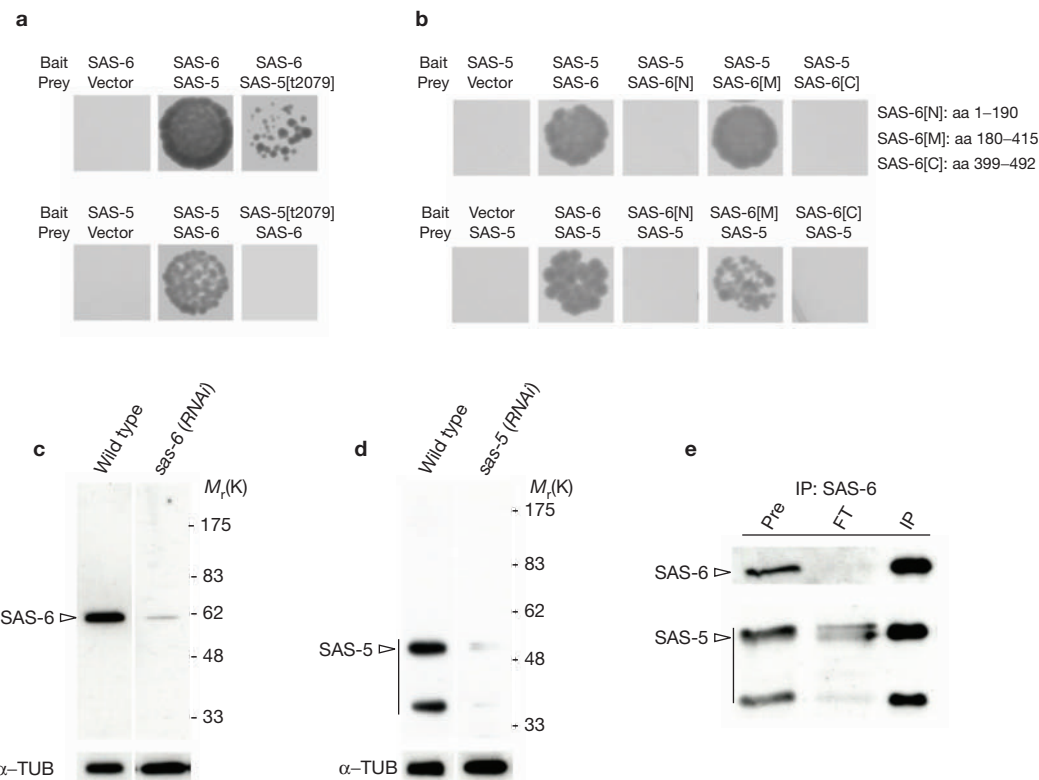


Figure 6 SAS-6 and SAS-5 physically interact. **(a, b)** Yeast two-hybrid assay testing interaction between full-length SAS-6 and SAS-5 or SAS-5[t2079] (**a**), as well as the indicated fragments of SAS-6 and full-length SAS-5 (**b**). We also found that SAS-5 interacts with itself, as well as with SAS-5[t2079] (data not shown). aa, amino acid. **(c, d)** Western blot analysis using SAS-6 (**c**) or SAS-5 (**d**) antibodies on embryonic extracts of the indicated genotypes. Note that SAS-5 antibodies detect two main species, one at the expected size as well as a smaller one, and that the larger species can be resolved further into a doublet following shorter exposure or when less material is

present (for example, *sas-5(RNAi)* lane). The membranes were reprobed with α-tubulin (α-TUB) antibodies as a loading control. **(e)** Wild-type embryonic extracts immunoprecipitated with SAS-6 antibodies and analysed by western blot using antibodies against SAS-5 or SAS-6, as indicated with the arrowheads. IP: immunoprecipitated material. The input (Pre) and unbound (FT) material (in each case, 1/15 of starting material) are shown as well. SAS-5 antibodies did not co-immunoprecipitate SAS-6 (data not shown), perhaps because the epitopes that are recognized by the SAS-5 antibodies are engaged in protein–protein interactions with SAS-6.

We also noted that transfection with GFP–HsSAS-6 results in 23% of U2OS cells harbouring more than two such foci, compared with 5% of cells following transfection with GFP alone (Fig. 7b–e; $n = 325$ and 310, respectively; $P < 0.0001$, Chi-square analysis). Excess foci are unlikely to result from defective cell division and consequent tetraploidization — as, for example, when Aurora-A is overexpressed¹⁹ — because most of the U2OS cells transfected with GFP–HsSAS-6 and bearing multiple foci are not multinucleated (see Fig. 7b–e; 90%, $n = 101$). In addition, excess foci do not seem to result from a block in cell-cycle progression, because bulk proliferation rates and FACS profiles of cells transfected with GFP–HsSAS-6 are not significantly different from those of cells transfected with GFP alone (Supplementary Fig. S1a–e). Moreover, time-lapse analysis established that the average duration of the cell cycle is not altered in cells expressing GFP–HsSAS-6 (Supplementary Fig. S1f–h). Accordingly, the frequency of mitotic figures with multipolar spindles is increased in such cells (Supplementary Fig. S1i–k; 19%, $n = 93$; compared with 5% in cells transfected with GFP alone, $n = 94$; $P < 0.001$, Chi-square analysis). Whereas additional experiments will be needed to ascertain the origin of the multiple foci, the findings so far indicate that overexpression of HsSAS-6 may result in an excess of centrioles.

We then tested whether HsSAS-6 is required for centrosome duplication, first using an overduplication assay. When otherwise normal U2OS cells are treated with the DNA polymerase α-inhibitor aphidicolin, centrosome overduplication ensues²⁰. As shown in Fig. 7f and 7g, we found that small interfering RNA (siRNA)-mediated inactivation of HsSAS-6 abrogates this effect, as only 38% of aphidicolin-treated U2OS cells contain ≥3 foci of C-Nap1, compared with 82% or 88% following treatment with control siRNAs directed against luciferase or lamin-B, respectively. We conclude that HsSAS-6 is required for efficient overduplication of centrosomes in aphidicolin-treated U2OS cells.

We next addressed whether HsSAS-6 also has a role in the normal centrosome duplication cycle of U2OS cells, focusing on mitotic cells to assay the number of centrosomes generated by the end of the duplication cycle. Strikingly, we found that siRNA-mediated inactivation of SAS-6 results in 44% of mitotic cells showing a monopolar spindle, with one focus of γ-tubulin and C-Nap1, whereas only 1% of control cells transfected with lamin-B siRNAs showed such characteristics (Fig. 7i–7k and data not shown). In addition, we noted signs of failed cytokinesis and cell death following treatment with HsSAS-6 siRNAs (data not shown). Overall, our findings establish that HsSAS-6 is required for progression through the centrosome duplication cycle in human cells.

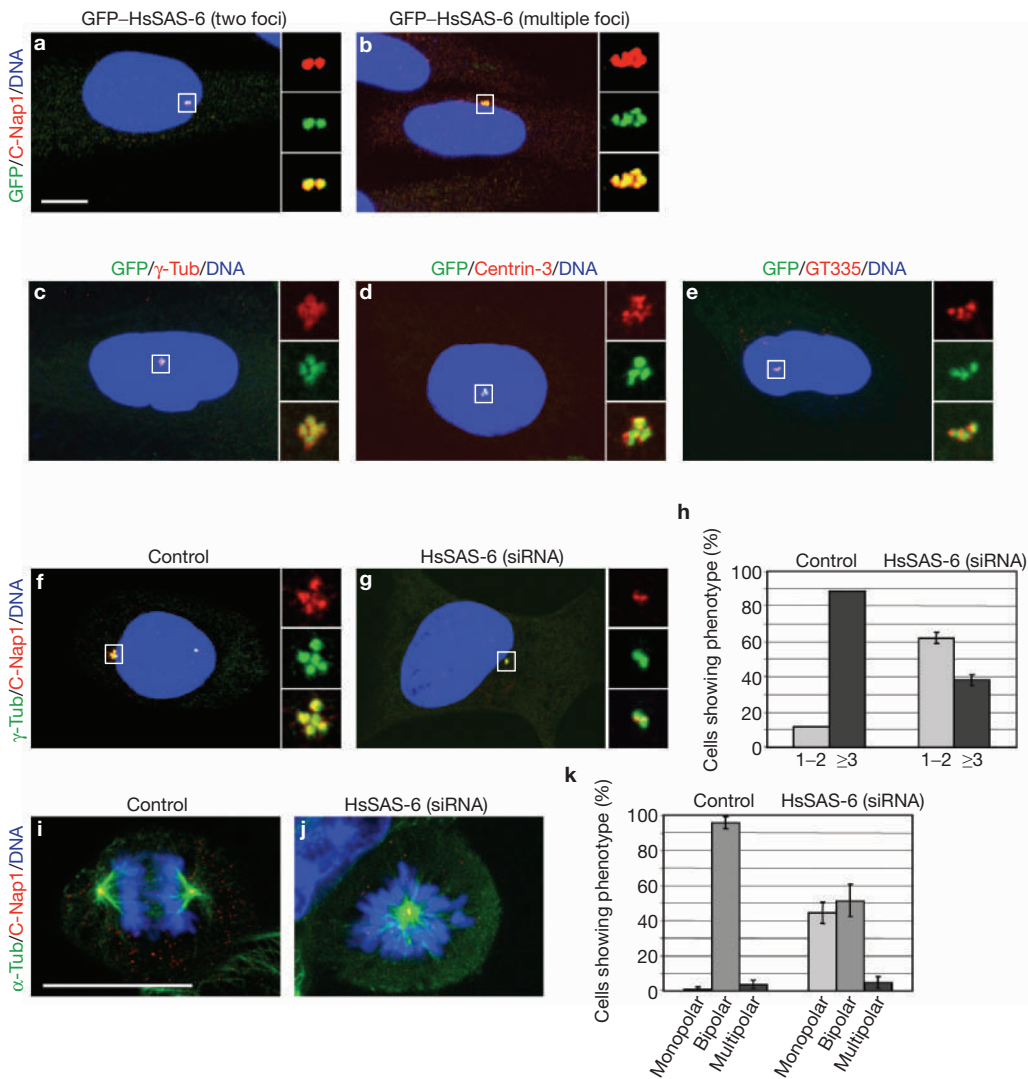


Figure 7 HsSAS-6 is required for centrosome duplication in human cells. **(a–e)** U2OS cells transfected with GFP–HsSAS-6, fixed 48 h thereafter, and stained with antibodies against C-Nap1 (**a, b**), γ -tubulin (**c**), centrin-3 (**d**), poly-glutamylated tubulin (GT335; **e**) (all red) and GFP (green); DNA is shown in blue. Insets in **(a–g)** are 3–7-fold magnified views. **(f, g)** U2OS cells mock-transfected (**f**) or transfected with small interfering (siRNAs) directed against HsSAS-6 (**g**) and treated 24 h later with aphidicolin for 72 h before fixation and staining with antibodies against C-Nap1 (red) and γ -tubulin (α -TUB; green); DNA is shown in blue. **(h)** Quantification of centriole number (1–2 or ≥ 3) in cells treated as in **f, g** and detected by anti-C-Nap1 staining. Shown are averages of two independent experiments for HsSAS-6 siRNAs, along with standard deviations, and one control experiment with control lamin-B siRNAs. The differences between cells transfected with siRNAs

directed against SAS-6 ($n=247$) and either lamin-B ($n=69$) or luciferase ($n=103$) (not shown in the graph; see text) are statistically significant (for both comparisons: $P<0.0001$, Chi-square analysis). **(i, j)** U2OS cells transfected with siRNAs directed against control lamin-B (**i**) or HsSAS-6 (**j**), fixed after 96 h and stained with antibodies against C-Nap1 (red) and α -tubulin (α -TUB; green); DNA is shown in blue. **(k)** Quantification of mitotic cells treated as in **i, j** and assembling a monopolar, bipolar or multipolar spindle, as detected by anti- α -tubulin and anti-C-Nap1 staining. Shown are averages of two experiments, along with standard deviations. The occurrence of a monopolar spindle is statistically significant ($n=161$ control; $n=69$ human SAS-6 siRNA-treated; $P<0.0001$, Chi-square analysis). Similar conclusions were reached by scoring cells 72 h after transfection, as well as by scoring spindle assembly using γ -tubulin and C-Nap1 (data not shown).

DISCUSSION

We identified SAS-6 as a novel protein that is required for daughter centriole formation in *C. elegans*. Our analysis of near-genome-wide RNAi data did not uncover components other than ZYG-1, SAS-4, SAS-5, SPD-2 and SAS-6. This indicates that these five proteins comprise the core components that can be identified through simple maternal-effect screens as being required for this step of the centrosome duplication cycle.

Our work clarifies the relationship between some of these components. First, we previously established that ZYG-1 is required

for the presence of SAS-5 at centrioles⁴; we now extend this observation to SAS-6. Second, we show that SAS-5 and SAS-6 physically interact and are mutually dependent for their centriolar distribution. As SAS-5 shuttles between the cytoplasm and centrioles, SAS-5 may act to target SAS-6 to centrioles. Third, we establish that SAS-6 is recruited to centrioles once per cell cycle, at the onset of the duplication cycle. A comparison of GFP–SAS-6 with GFP–SAS-4 using FRAP analysis (ref. 3) indicates that GFP–SAS-6 may be recruited slightly before GFP–SAS-4. Moreover, we

found that GFP-SAS-6 recruitment occurs at mother centrioles independently of SAS-4, but that its continued presence at centrioles requires SAS-4, raising the possibility that SAS-6 normally associates with the emerging daughter centriole. Together, these findings indicate a working model in which ZYG-1 acts on SAS-5/SAS-6, thereby allowing SAS-6 recruitment to the mother centriole, which in turn enables SAS-4 loading and daughter centriole formation.

SAS-6 is the founding member of an evolutionarily conserved protein family with a conserved PISA motif. Interestingly, a single PISA-containing protein is present in eukaryotes that have basal bodies or centrioles, whereas none are apparent in budding or fission yeast, which have structurally distinct spindle-pole bodies instead of centrosomes. The PISA motif does not resemble other signature sequences, but the invariable pairing with a coiled-coil domain indicates that the two protein features may act together. The mechanisms by which SAS-6 and other PISA-containing proteins regulate centrosome biogenesis are not known. Because HsSAS-6 overexpression yields excess foci containing centriolar proteins, it is tempting to speculate that HsSAS-6 has organizing capacity for centriole formation. This observation mirrors one made in *C. elegans*, in which partial RNAi-mediated inactivation of *sas-6* results in intermediate phenotypes that — in the case of *sas-4(RNAi)* — reflect partially formed centrioles². These observations raise the possibility that PISA-containing proteins are dose-dependent regulators of basal body or centriole formation.

Before this work, it was not clear whether findings made in *C. elegans* have molecular bearings on the mechanisms of centrosome duplication in other organisms⁷. Here, we show that HsSAS-6 is required for progression through the centrosome duplication cycle of human cells. Human centrosomal proteins that are required for centriole reproduction include centrin-2 and the polo-like kinase PLK-2 (refs 9,21). However, there is no apparent centrin gene in nematodes⁷, and even though the *C. elegans* PLK-1 localizes to centrosomes in early embryos, it is not required for centrosome duplication²². Therefore, our work provides the first evidence that molecules ensuring centrosome duplication have been functionally conserved through the evolution of worms to humans. Such broad conservation makes it more likely that the postulated distant human relatives of SAS-4 (ref. 3) and SPD-2 (ref. 6) may be similarly required. As aberrant control of centrosome number is thought to contribute to tumorigenesis²³, further understanding of the mechanism of action of *C. elegans* SAS-6 and HsSAS-6 may also hold important diagnostic and therapeutic potential for cancer biology.

Note added in proof: While this manuscript was under review, another study reported the characterization of *C. elegans* SAS-6 (ref. 24).

ACKNOWLEDGEMENTS

We are especially grateful to X. Yan, R. Habedanck and E. Nigg for guidance with cell culture techniques and reagents, as well as M. Cockell for help in generating SAS-6 fusion proteins. We thank J. Azimsadeh, M. Bornens, B. Eddé, M. Glotzer and V. Simanis for reagents. C. Echeverri is acknowledged for communicating results before publication; R. Iggo, V. Simanis and P. Strnad for critical reading of the manuscript; M. Migliaccio, P. Strnad and A. Wilson for help with FACS analysis; C. Bonnard and N. Garin for microscopy support; and D. Moersch and I. Jouravleff for helpful discussions. Some strains were obtained from the *Caenorhabditis* Genetics Center, which is funded by the National Institute of Health National Center for Research Resources (NCRR). M. D. is recipient of a Roche Research Foundation postdoctoral fellowship. Oncosuisse supports work on centrosome duplication in the Gönczy laboratory (OCS-01495-02-2004).

METHODS

Nematodes. Nematode culture was carried out according to standard procedures²⁵. The strains *zyg-1(b1)* II (ref. 26), *sas-5(t2079)* V (ref. 4) and *fem-1(hc17)* IV (ref. 27) were utilized as previously described⁴. Other strains used were GFP-TAC-1 (ref. 17), GFP-SAS-4 (ref. 2) and GFP-SAS-5 (ref. 4). *sas-4(RNAi)* and *sas-5(RNAi)* were generated as described previously^{3,4}. *sas-4(RNAi)* and *sas-5(RNAi)* were used under severe inactivation conditions that did not yield asymmetric spindles, and, therefore, partially formed centrioles². For *sas-6(RNAi)*, the entire genomic sequence was cloned into L4440 (ref. 28), and RNAi was performed by placing L4 larvae on a feeding plate at 20 °C for >24 h. Partial *sas-6* inactivation was achieved as described previously, fixing embryos starting 12 h after the onset of feeding and scoring all blastomeres at the two-cell stage⁴.

For generation of GFP-SAS-6 transgenic animals, appropriate primers (the sequence of these and all other primers are available on request) were used to PCR-amplify *sas-6* genomic DNA, replacing the first ATG by CTG. The sequence-verified fragment was cloned into pSU25, a *pie-1*-based vector containing a rescuing *unc-119* cDNA (a gift from Michael Glotzer). The plasmid was sequence-verified and bombarded²⁹, yielding two integrated strains of genotype *unc-119(ed3)* is18 {pSL445;*pie-1-GFP-SAS-6(Y45F10D.9)*} . In contrast to GFP-SAS-4 and GFP-SAS-5 (refs 2–4), GFP-SAS-6 is essentially not expressed in male germ cells.

***sas-6* gene structure and bioinformatic analysis.** RNA from mixed developmental stages was prepared for reverse transcription PCR (RT-PCR) reactions (Qiagen, Hilden, Germany) using SL1 or SL2 forward primers and a reverse primer at the 3'-end of the gene. The products were used as template for nested PCR, using SL1 or SL2 forward primers and a different reverse primer, yielding a fragment of the expected size with SL1, which was cloned into pGEMTEasy (Promega, Madison, WI) and sequenced, yielding a sequence identical to that predicted by WormBase (www.wormbase.org/; freeze WS130).

The N-terminal region of SAS-6 was used to find homologous sequences in Swiss-Prot, TrEMBL, TrGEN, TrEST, trome and ENSEMBL, using iterative BLAST³⁰ (<http://myhits.isb-sib.ch/>). After four rounds of PSI-BLAST using standard parameters, we defined a motif of ~50 amino acids found in Q80UK7 and Q9CYT4 (mouse), Q6UVJ0 (human), Q7ZVT3 (zebrafish), RTR015060 (rat), Q6NRG6 (frog), Cin_2205_1 (ascidian), BG785391 (sea urchin), ENSCBRP00000004941 (*Caenorhabditis briggsae*), O62479 (*C. elegans*), AJ456816 (chicken) and Q6LFJ0 (plasmid). From the multiple alignment of the motif, a profile was derived using PfTools³¹ (semi-global mode, BLOSUM45). After calibration on a protein set based on shuffled sequences, the profile was used to search Swiss-Prot and TrEMBL. All proteins that were detected with both the PSI-BLAST and profile method were further analysed for coiled-coil regions using the COILS and MARCOIL software (<http://www.ch.embnet.org/>). Pairwise alignments and dot plots were used to confirm the similar domain organization between potential homologous proteins.

For *Chlamydomonas reinhardtii*, we searched the full genome (chlre2 from [ftp.jgi-psf.org](http://jgi-psf.org/)) using TBLASTN and the PISA motif of the mouse protein Q80UK7 as query. We found a match on the reverse strand of the *Chlamydomonas* scaffold_16 genomic sequence at position 664195–664377. The full protein structure has been predicted with GenScan (<http://genes.mit.edu/GENSCAN.html>) using the region 663000–664400 of the scaffold_16 sequence.

Antibodies and indirect immunofluorescence on embryos. Full-length *sas-6* cDNA was cloned into pGEX-6P-3 (Amersham Pharmacia Biotech, Freiburg, Germany) to express GST-SAS-6, which was purified from SDS gels and injected into a rabbit according to standard procedures (Eurogentec, Seraing, Belgium). For affinity purification, full-length *sas-6* was cloned into a modified pET30a⁺ vector to express His(6)-SAS-6, as described previously³². Antibodies were affinity-purified using His(6)-SAS-6, eluting with 0.1 M glycine at pH 2.3. Antibodies were dialysed against phosphate-buffered saline (PBS) overnight at 4 °C and stored at -20 °C in 50% glycerol. SAS-5 antibodies for western blot analysis were affinity-purified in the same manner, using a previously described serum⁴.

Embryos were methanol-fixed, leaving slides in methanol for <10 min for detecting most centriolar antigens, <8 min for detecting SAS-6, and processed as described previously³. Primary antibodies were 1:200 mouse anti-tubulin (DM1A, Sigma, St Louis, MO); 1:100 rabbit anti-TAC-1 (ref. 16); 1:800 rabbit anti-SAS-4 (ref. 3); 1:20 rabbit anti-SAS-5 (ref. 4); 1:50 rabbit anti-SAS-6 (this study); 1:250 mouse anti-GFP (Chemikion International, Temecula, CA);

1:1000 mouse anti- γ -tubulin (GTU-88; Sigma); 1:1000 rabbit anti-C-Nap1 (a gift from Erich Nigg)³³; 1:1000 rabbit anti-centrin-3 (a gift from Juliette Azimsadeh and Michel Bornens)³⁴; 1:1000 mouse anti-polyglutamylated tubulin (GT335, a gift from Bernard Eddé)¹⁷. Slides were counterstained with ~1 $\mu\text{g ml}^{-1}$ Hoechst 33258 (Sigma) to reveal DNA. Secondary antibodies coupled to Alexa488 (Molecular Probes, Eugene, OR) or Cy3 (Dianova, Hamburg, Germany) were used at 1:1000.

Microscopy. Dual time-lapse DIC, fluorescence microscopy, spinning disc time-lapse confocal microscopy and FRAP analysis were performed as described previously⁴. Indirect immunofluorescence was imaged on an LSM 510 Zeiss confocal microscope, using 0.6–1.2 μm optical slices. Images were processed using Adobe Photoshop. For Fig. 3g, the insets were deconvolved using Imaris (Bitplane, Zurich, Switzerland) with standard settings.

Yeast two-hybrid and co-immunoprecipitation experiments. Yeast strain MAV105 was grown in YPD medium and transformed with vectors pPC86 and pPC97 (Clontech, BD Biosciences, San Jose, CA). Positive colonies were grown in yeast drop-out medium (−L−W) overnight as described previously¹⁷, after which cells were diluted to OD₅₉₅ = 1.6 μl of this stock. In addition, two serial dilutions of these cells were made to ODs of 0.1 and 0.01, respectively, which were spotted on yeast (−L−W) plates supplemented with 20 mM 3-Amino-Triazol. Plates were placed at 30 °C and grown until clear colonies formed with a positive control (ZYG-8/TAC-1 in the initial experiments¹⁷ and SAS-6/SAS-5 in subsequent ones).

Fragments of SAS-5 and SAS-6 were obtained following PCR amplification using appropriate primer pairs, followed by sequence verification. SAS-5[t2079] was generated using PCR-mediated mutagenesis and were then sequence-verified.

Co-immunoprecipitation experiments with wild-type embryonic extracts were carried out as described previously³⁵.

Cell culture and transfection. U2OS cells were cultured at 37 °C and 5% CO₂ in high glucose DMEM supplemented with GlutaMAX (Invitrogen, Carlsbad, CA), supplemented with 100 units/ml penicillin, 100 $\mu\text{g ml}^{-1}$ streptomycin and 10% fetal calf serum (Sigma).

Full-length human SAS-6 cDNA was obtained by PCR amplification of two overlapping fragments present in the partial cDNAs DKFZp761A078Q and IRALp96J2248Q. After sequence verification, the two fragments were fused and cloned into pEGFP-C1 (Clontech). U2OS cells were transfected using FUGENE6 (Roche, Rotkreuz, Switzerland) according to the manufacturer's protocol. Briefly, cells were split 24 h before transfection and seeded to a density of ~1 \times 10⁵ cells/well in six-well plates on coverslips. 3 μl of FUGENE6 reagent was used with 0.5 μg or 1 μg of DNA. Examination of GFP fluorescence indicated a transfection efficiency of approximately 40%.

For inactivation of HsSAS-6, three double-stranded RNA oligonucleotides with the sequences CAAGAGGUAGCAAAUUCACUU (siRNA1), GAAAGGACUUAGUUUUCGUU (siRNA2) and GCACGUUAAUCAGCUACAUU (siRNA3) were ordered from the siGENOME collection (Dharmacon, Lafayette, CO) and diluted to 20 μM in 1× Oligo Buffer provided by the manufacturer. U2OS cells were split 24 h before transfection and seeded as above. Just before transfection, the medium was exchanged against 1 ml DMEM lacking antibiotics. 6 μl of a 1:1:1 solution of siRNA duplexes was mixed with 100 μl OptiMEM medium (Invitrogen), as well as 3 μl Oligofectamine (Invitrogen) with 27 μl OptiMEM. The two mixes were then combined, incubated for 15–20 min at room temperature and added to the wells. 24 h later, 1 ml of medium was added to the wells. For the centrosome overduplication assay, 2 μl aphidicolin (1.6 mg ml^{-1} in DMSO; Sigma) was added at the same time. Treatment with siRNA3 alone resulted in indistinguishable results from those obtained with the 1:1:1 mixture; treatment with siRNA2 alone resulted in an intermediate abrogation of centrosome overduplication; treatment with siRNA1 alone was indistinguishable from control cells (data not shown).

Indirect immunofluorescence on tissue culture cells. Coverslips were removed and washed in PBS. Cold (~20 °C) methanol was added and the cells were transferred to ~20 °C for ~10 min. Methanol was removed, the coverslips washed in PBS and blocked for 20 min in 1% bovine serum albumin (BSA) in PBS. Primary antibodies were diluted in 1% BSA in PBS, incubated at 4 °C for >3 h

and coverslips washed four times in PBS. Secondary antibodies were diluted in 1% BSA in PBS at ~1 $\mu\text{g ml}^{-1}$ Hoechst 33258, and the coverslips incubated for 45 min at room temperature and washed again four times in PBS. Excess PBS was blotted on a paper towel and coverslips were mounted on slides.

Cells were analysed with a \times 100 lens for the presence of discrete C-Nap1- or GT335-positive foci. For U2OS cells transfected with GFP-SAS-6, all cells were scored regardless of GFP being detected or not, such that the proportion of transfected cells with multiple C-Nap1-positive foci given in the text is probably an underestimate.

- O'Connell, K.F. et al. The *C. elegans* zyg-1 gene encodes a regulator of centrosome duplication with distinct maternal and paternal roles in the embryo. *Cell* **105**, 547–558 (2001).
- Kirkham, M., Müller-Reichert, T., Oegema, K., Grill, S. & Hyman, A.A. SAS-4 is a *C. elegans* centriolar protein that controls centrosome size. *Cell* **112**, 575–587 (2003).
- Leidel, S. & Gönczy, P. SAS-4 is essential for centrosome duplication in *C. elegans* and is recruited to daughter centrioles once per cell cycle. *Dev. Cell* **4**, 431–439 (2003).
- Delattre, M. et al. Centriolar SAS-5 is required for centrosome duplication in *C. elegans*. *Nature Cell Biol.* **6**, 656–664 (2004).
- Kemp, C.A., Kopish, K.R., Zipperlen, P., Ahringer, J. & O'Connell, K.F. Centrosome maturation and duplication in *C. elegans* require the coiled-coil protein SPD-2. *Dev. Cell* **6**, 511–523 (2004).
- Pelletier, L. et al. The *Caenorhabditis elegans* centrosomal protein SPD-2 is required for both pericentriolar material recruitment and centriole duplication. *Curr. Biol.* **14**, 863–873 (2004).
- Azimsadeh, J. & Bornens, M. in *Centrosomes in Development and Disease* (ed. Nigg, E.A.) 93–122 (Wiley-VCH, Weinheim, 2004).
- Wolf, N., Hirsh, D. & McIntosh, J.R. Spermatogenesis in males of the free-living nematode, *Caenorhabditis elegans*. *J. Ultrastruct. Res.* **63**, 155–169 (1978).
- Salisbury, J.L., Suino, K.M., Busby, R. & Springett, M. Centrin-2 is required for centriole duplication in mammalian cells. *Curr. Biol.* **12**, 1287–1292 (2002).
- Dutcher, S.K. & Trabuco, E.C. The UN13 gene is required for assembly of basal bodies of *Chlamydomonas* and encodes δ -tubulin, a new member of the tubulin superfamily. *Mol. Biol. Cell* **9**, 1293–1308 (1998).
- Dutcher, S.K., Morrisette, N.S., Preble, A.M., Rackley, C. & Stanga, J. ϵ -tubulin is an essential component of the centriole. *Mol. Biol. Cell* **13**, 3859–3869 (2002).
- Garreau de Loubresse, N., Ruiz, F., Beisson, J. & Klötz, C. Role of δ -tubulin and the C-tubule in assembly of *Paramecium* basal bodies. *BMC Cell Biol.* **2**, 4 Epub 2001 Mar 07 (2001).
- Hung, L.Y., Tang, C.J. & Tang, T.K. Protein 4.1 R-135 interacts with a novel centrosomal protein (CPAP) which is associated with the γ -tubulin complex. *Mol. Cell. Biol.* **20**, 7813–7825 (2000).
- Andersen, J.S. et al. Proteomic characterization of the human centrosome by protein correlation profiling. *Nature* **426**, 570–574 (2003).
- Piano, F., Schetter, A.J., Mangone, M., Stein, L. & Kemphues, K.J. RNAi analysis of genes expressed in the ovary of *Caenorhabditis elegans*. *Curr. Biol.* **10**, 1619–1622 (2000).
- Sönichsen, B. et al. Full genome RNAi profiling of early embryogenesis in *C. elegans*. *Nature* (in the press).
- Bellanger, J.M. & Gönczy, P. TAC-1 and ZYG-9 form a complex that promotes microtubule assembly in *C. elegans* embryos. *Curr. Biol.* **13**, 1488–1498 (2003).
- Wolff, A. et al. Distribution of glutamylated α and β -tubulin in mouse tissues using a specific monoclonal antibody, GT335. *Eur. J. Cell Biol.* **59**, 425–432 (1992).
- Meraldi, P., Honda, R. & Nigg, E.A. Aurora-A overexpression reveals tetraploidization as a major route to centrosome amplification in p53^{−/−} cells. *EMBO J.* **21**, 483–492 (2002).
- Meraldi, P., Lukas, J., Fry, A.M., Bartek, J. & Nigg, E.A. Centrosome duplication in mammalian somatic cells requires E2F and Cdk2-cyclin A. *Nature Cell Biol.* **1**, 88–93 (1999).
- Warnke, S. et al. Polo-like kinase-2 is required for centriole duplication in mammalian cells. *Curr. Biol.* **14**, 1200–1207 (2004).
- Chase, D. et al. The polo-like kinase PLK-1 is required for nuclear envelope breakdown and the completion of meiosis in *Caenorhabditis elegans*. *Genesis* **26**, 26–41 (2000).
- Pihan, G.A., Wallace, J., Zhou, Y. & Doxsey, S.J. Centrosome abnormalities and chromosome instability occur together in pre-invasive carcinomas. *Cancer Res.* **63**, 1398–1404 (2003).
- Demmermann, A., Müller-Reichert, T., Pelletier, L., Habermann, B., Desai, A. & Oegema, K. Centriole assembly requires both centriolar and pericentriolar material proteins. *Dev. Cell* **7**, 815–829 (2004).
- Brenner, S. The genetics of *Caenorhabditis elegans*. *Genetics* **77**, 71–94 (1974).
- Wood, W.B. et al. Parental effects and phenotypic characterization of mutations that affect early development in *Caenorhabditis elegans*. *Dev. Biol.* **74**, 446–469 (1980).
- Nelson, G.A., Lew, K.K. & Ward, S. Intersex, a temperature-sensitive mutant of the nematode *Caenorhabditis elegans*. *Dev. Biol.* **66**, 386–409 (1978).
- Timmons, L., Court, D.L. & Fire, A. Ingestion of bacterially expressed dsRNAs can produce specific and potent genetic interference in *Caenorhabditis elegans*. *Gene* **263**, 103–112 (2001).
- Praitis, V., Casey, E., Collar, D. & Austin, J. Creation of low-copy integrated transgenic lines in *Caenorhabditis elegans*. *Genetics* **157**, 1217–1226 (2001).
- Pagni, M. et al. MyHits: a new interactive resource for protein annotation and domain identification. *Nucleic Acids Res.* **32**, W332–W335 (2004).

31. Sigrist, C.J. *et al.* PROSITE: a documented database using patterns and profiles as motif descriptors. *Brief Bioinform.* **3**, 265–274 (2002).
32. Braun, P. *et al.* Proteome-scale purification of human proteins from bacteria. *Proc. Natl Acad. Sci. USA* **99**, 2654–2659 (2002).
33. Fry, A.M. *et al.* C-Nap1, a novel centrosomal coiled-coil protein and candidate substrate of the cell cycle-regulated protein kinase Nek2. *J. Cell Biol.* **141**, 1563–1574 (1998).
34. Middendorp, S. *et al.* A role for centrin 3 in centrosome reproduction. *J. Cell Biol.* **148**, 405–416 (2000).
35. Pintard, L. *et al.* The BTB protein MEL-26 is a substrate-specific adaptor of the CUL-3 ubiquitin-ligase. *Nature* **425**, 311–316 (2003).
36. Clamp, M., Cuff, J., Searle, S.M. & Barton, G.J. The Jalview Java alignment editor. *Bioinformatics* **20**, 426–427 Epub 2004 Jan 2022 (2004).

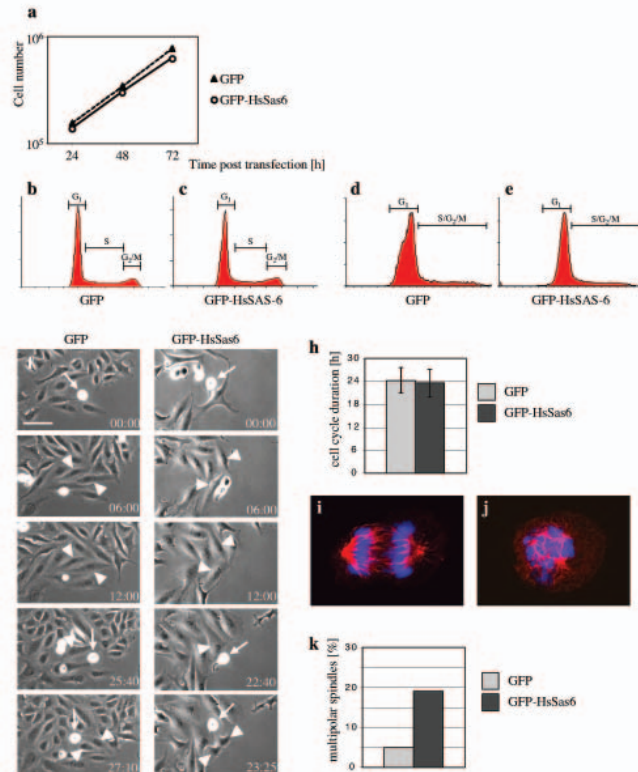


Figure S1 (a) Bulk cell proliferation assay. Approximately 0.4×10^5 U2OS cells were seeded on several 6cm diameter dishes and transfected 24h later with GFP or GFP-HsSAS-6. After an additional 24h, 48h or 72h, cells in one dish per construct were harvested and cell number determined using a Neubauer counting chamber. Note that experimental and control cell populations have identical proliferation profiles. (b-e) FACS analysis. Cells were grown in 10 cm dishes, transfected with GFP or GFP-HsSAS-6 and processed for immunofluorescence and FACS analysis 48 hours after transfection. For analysis, cells were gated to remove doublets and debris. For FACS analysis with propidium iodide (PI) (b, c), cells were trypsinized and washed in PBS. Cold 70% Ethanol was added drop-wise to pellets, cells left at 4 °C for 30min and then washed 2x in PBS. 50µl of 100µg/ml RNaseA (Sigma) was added and the cells incubated at 37 °C for 1h. 200µl of 50µg/ml propidium iodide (Sigma) was then added and cells analyzed using CellQuest on a BD FACScan. The fraction of cells in the different phases of the cell cycle (as indicated in the figure) were as follows: G1, 64% (GFP) and 67% (GFP-HsSAS-6); S: 21% (GFP) and 19% (GFP-HsSAS-6); G2/M: 15% (GFP) and 15% (GFP-HsSAS-6). For bi-parametric FACS analysis with GFP/Hoechst (d, e), cells were trypsinized, washed in PBS-3%FCS, incubated with Hoechst 33342 (Sigma) for 10min at room temperature and analyzed on a BD-LSR. Live cells were divided into groups of no/low, medium and high expression levels of GFP. Only cells with medium expressing levels are shown, but FACS profiles of cells with no/low and high expression levels of GFP were analogous. The fraction of cells in G1 versus the remainder of the cell cycle (as indicated in the figure) were as follows: G1, 77% (GFP) and 71% (GFP-HsSAS-6); S/G2/M: 25% (GFP) and 20% (GFP-HsSAS-6). (f-h) Live analysis of cell cycle progression. U2OS cells placed in a 6-well dish were transfected as in (a) and transferred 24h later to a homemade incubator chamber on an automated Zeiss Axioplan 100 microscope. The chamber was heated at 37 °C, supplemented with ~5% CO₂ and the medium was supplemented with 20mM HEPES pH 7.5. Infrared phase-images were taken through a 10x lens every 5 minutes at 5 different locations for each condition during 48 hours, controlled by Metamorph software (Universal). At the end of the sequence, a fluorescent image was taken for each of the 10 positions to reveal cells expressing GFP and thus restrict analysis to transfected cells. Cells with intermediate GFP levels were chosen as they displayed most consistently excess foci in the immunofluorescence analysis and their cell cycling time analyzed using the time-lapse recordings. Shown are 5 images from a time-lapse sequence of cells transfected with GFP (f) or GFP-HsSAS-6 (g); scale bar is 50 µm. Arrows point to relevant cells in mitosis, arrowheads to their daughters; elapsed time is shown in hours and min. Note that the average duration of the cell cycle is statistically indistinguishable when comparing cells transfected with GFP or GFP-HsSAS-6 (h; n=19 and 18, respectively; p>0.26; Student's T-test). (i-k) U2OS cells transfected with GFP (i) or GFP-HsSAS-6 (j) were fixed 48 hours thereafter and stained with antibodies against α-tubulin (red); DNA is shown in blue. Note bipolar spindle in (i) and multipolar spindle in (j); scale bar is 10 µm. Shown also is the incidence of multipolar spindles in U2OS cells transfected with GFP or GFP-HsSAS-6 and stained with antibodies against poly-glutamylated tubulin to accurately score spindle poles (k).

HsSAS-6); S/G2/M: 25% (GFP) and 20% (GFP-HsSAS-6). (f-h) Live analysis of cell cycle progression. U2OS cells placed in a 6-well dish were transfected as in (a) and transferred 24h later to a homemade incubator chamber on an automated Zeiss Axioplan 100 microscope. The chamber was heated at 37 °C, supplemented with ~5% CO₂ and the medium was supplemented with 20mM HEPES pH 7.5. Infrared phase-images were taken through a 10x lens every 5 minutes at 5 different locations for each condition during 48 hours, controlled by Metamorph software (Universal). At the end of the sequence, a fluorescent image was taken for each of the 10 positions to reveal cells expressing GFP and thus restrict analysis to transfected cells. Cells with intermediate GFP levels were chosen as they displayed most consistently excess foci in the immunofluorescence analysis and their cell cycling time analyzed using the time-lapse recordings. Shown are 5 images from a time-lapse sequence of cells transfected with GFP (f) or GFP-HsSAS-6 (g); scale bar is 50 µm. Arrows point to relevant cells in mitosis, arrowheads to their daughters; elapsed time is shown in hours and min. Note that the average duration of the cell cycle is statistically indistinguishable when comparing cells transfected with GFP or GFP-HsSAS-6 (h; n=19 and 18, respectively; p>0.26; Student's T-test). (i-k) U2OS cells transfected with GFP (i) or GFP-HsSAS-6 (j) were fixed 48 hours thereafter and stained with antibodies against α-tubulin (red); DNA is shown in blue. Note bipolar spindle in (i) and multipolar spindle in (j); scale bar is 10 µm. Shown also is the incidence of multipolar spindles in U2OS cells transfected with GFP or GFP-HsSAS-6 and stained with antibodies against poly-glutamylated tubulin to accurately score spindle poles (k).

SUPPLEMENTARY INFORMATION

Movies 1 and 2 Dual GFP fluorescence and DIC time-lapse recordings of wild-type (Movie 1) or *sas-6(RNAi)* (Movie 2) embryos expressing GFP-TAC-1, from the time of pronuclear formation until the end of the second cell cycle. Images were captured every 10 seconds and the display rate is 10 frames per second; elapsed time indicated in minutes and seconds. Note that the intensity of GFP-TAC-1 signal is maximal during mitosis, and that centrosomes are not always in focus.

Movie 3 Spinning disc confocal time-lapse recording of a one-cell stage embryo expressing GFP-SAS-6, from the time of pronuclear formation until the end of the first cell cycle. Six confocal slices ~1 μm -apart were captured every 15 seconds and a movie reconstructed by choosing at each time-point two neighboring focal planes containing centrioles. Display rate is 10 frames per second; elapsed time indicated in minutes and seconds. Note that centrioles in both centrosomes are not in focus in all images.